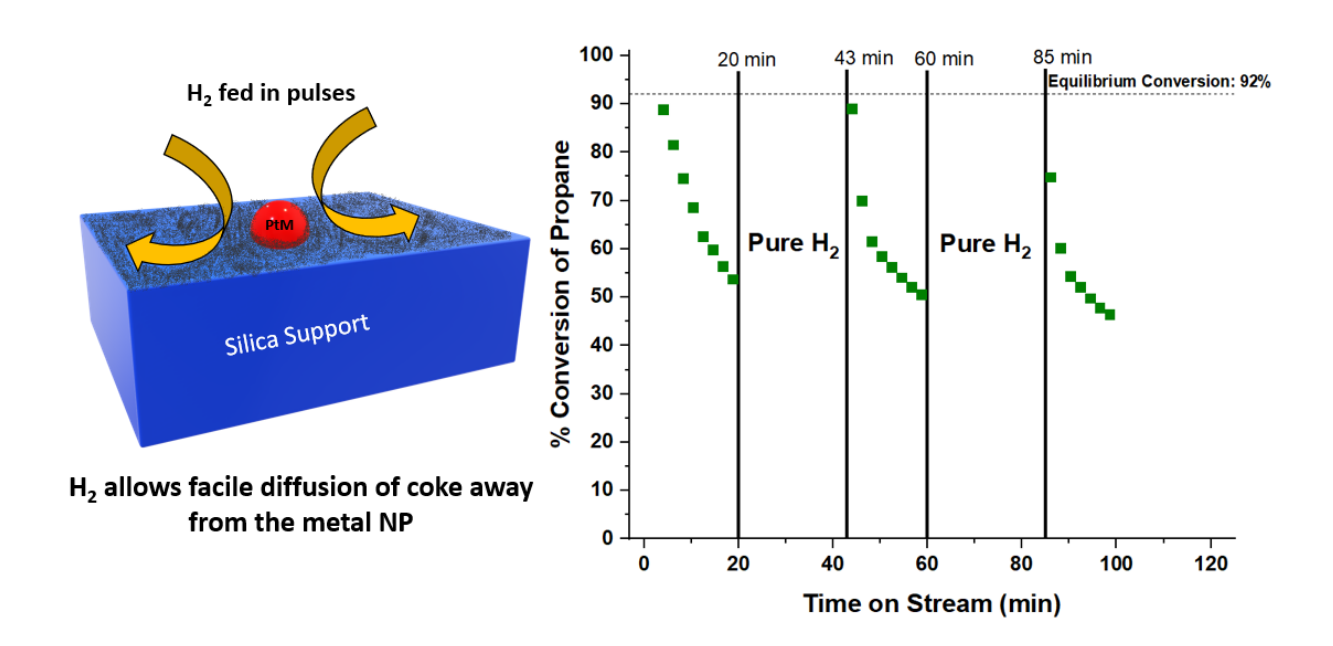
Alcala, R., Dean, D. P, Chavan, I., Chang, C.-W., Burnside, B., Pham, H. N., Peterson, E., Miller, J. T., Datye, A. K., Strategies for Regeneration of Pt-Alloy Catalysts Supported on Silica for Propane Dehydrogenation, Appl. Catal. A: Gen., 658 (2023) 119157, 10.1016/j.apcata.2023.119157.

# Strategies for Regeneration of Pt-alloy Catalysts Supported on Silica for Propane Dehydrogenation

Ryan Alcala<sup>1</sup>, David Dean<sup>2</sup>, Isha Chavan<sup>2</sup>, Che Wei Chang<sup>2</sup>, Brandon Burnside<sup>1</sup>, Hien Pham<sup>1</sup>, Eric Peterson<sup>1</sup>, Jeffrey T. Miller<sup>2, \*</sup>, and Abhaya Datye<sup>1,\*</sup>

<sup>\*</sup>Address for correspondence and proofs: datye@unm.edu



<sup>&</sup>lt;sup>1</sup>Department of Chemical and Biological Engineering and Center for Microengineered Materials, University of New Mexico, Albuquerque, New Mexico 87131, USA

<sup>&</sup>lt;sup>2</sup>Davidson School of Chemical Engineering, Purdue University, 480 Stadium Mall Drive, West Lafayette, IN 47907-2100, USA

#### **Abstract**

Catalyst stability, resistance to deactivation, and regeneration remains a challenge for high temperature reaction processes. For Pt alloys used in propane dehydrogenation (PDH), the primary pathways of catalyst deactivation include coke formation and metal nanoparticle sintering over time. Recent work shows that silica-supported catalysts provide excellent selectivity for this reaction, but the regenerability of silica-supported catalysts has not been established. In this work, we studied a series of Pt alloys including PtMn, PtZn, and PtSn, and tested them in the PDH reaction at 550 °C and 600 °C and subjected them to regeneration over multiple cycles. While oxidation in air restores the reactivity completely, with minimal catalyst sintering, it was surprising to see that these catalysts could also be regenerated in pure hydrogen. Here we explore the types of coke formed on these catalysts using *in situ* temperature programmed oxidation (TPO). Two types of coke were found. One on the metallic NP surface and a second type forms on the support. Our work shows that treatment in hydrogen causes redistribution of the coke between the metal and support, which can restore most of catalytic activity lost during reaction. The periodic introduction of H<sub>2</sub> during a reaction cycle may constitute an unexplored strategy for extending the lifetime of PDH catalysts.

## 1. Introduction

The "Shale Boom" has provided a large chemical feedstock of hydrocarbon resources that have a high hydrogen to carbon ratio, and the extraction of shale gas in the U.S. is projected to increase until at least 2050 [1–3]. Conversion of the natural gas liquids obtained from shale, for example, ethane and propane, involves dehydrogenation as the first step. The product alkenes are precursors for a variety of useful compounds including chemical derivatives and liquid transportation fuels. However, methane, ethane, and propane, the major components of natural gas, are difficult to activate, and dehydrogenation is a highly endothermic, equilibrium-limited reaction. Conventionally, Pt alloys or CrO<sub>x</sub> based catalysts supported on alumina have been employed for commercial dehydrogenation [4]. For non-oxidative dehydrogenation, when Pt is alloyed with another transition metal, the resulting alloy is very active and selective but still deactivates [5]. The mechanisms for deactivation include sintering of metal nanoparticles, coking of catalyst active sites, and the transformation of the active surface phase by loss of promoters [3]. The methods for catalyst regeneration on alumina supported catalysts are well developed and, in fact, commercial

processes are designed around the regeneration protocol involving fluidized beds (Dow FcDH process), alternating reactors (Catofin process), or a moving bed that undergoes continuous regeneration (UOP Oleflex process) [4,6].

Commercial processes for PDH involve operation from seconds to weeks with periodic oxidative regeneration [4]. It has been shown in the literature that over time, and periodic redox cycling at high temperatures, the most commonly used PtSn alloy supported on alumina deactivates by leaching of Sn out of the alloy, forming SnO<sub>x</sub> on the support (in addition to coking) [5]. Therefore, it would be beneficial to explore strategies for partially or completely avoiding oxidative regeneration, which is one of the goals of this work. Based on DFT and experimental studies, it was found that when hydrogen is cofed to the reaction, the catalyst exhibits higher stability and activity [7–14]. This is a form of coke suppression by which the increase in partial pressures of H<sub>2</sub> leads to a lower coverage of deeply dehydrogenated precursors on the surface (i.e., CCH<sub>3</sub> ethylidyne and CH methylidyne) by competing for active sites as well as preventing the readsorption of nascent propylene. Additionally, the higher the H<sub>2</sub> coverage, the lower the propylene adsorption strength and the higher the barrier for further dehydrogenation of propylene [7]. This is a remarkable and counterintuitive effect that is responsible for the high activity/stability of Pt-alloy (metal ensemble) when H<sub>2</sub> is cofed to the reaction and is now well-established in the literature. The question arises, could hydrogen be used to regenerate the catalyst?

Co-feeding H<sub>2</sub>, however, limits equilibrium conversion, so the ratio of H<sub>2</sub> to alkane feed should be optimized to balance stability and high yields [8]. In this work, we explore methods to address catalyst deactivation through the use of H<sub>2</sub> to regenerate the catalyst, alleviating the need for frequent oxidative regeneration [4]. Our strategy for achieving catalyst stability and regeneration involves cofeeding hydrogen to the catalyst either continuously or in pulses, providing an alternative approach to the propane dehydrogenation reaction typically done in industry. We studied three alloy catalysts, PtMn, PtSn, and PtZn, which have previously been reported to be active and selective for propane dehydrogenation [5,15–20].

Typically, catalysts used in commercial processes are supported on alumina due to its thermal stability, high surface area, the ability to regenerate the catalyst through oxidative regeneration [5]. However, recent work shows that silica supports may provide lower deactivation rates, better selectivity, but the regenerability of silica supports has not been well established [21–26]. The mechanisms for deactivation which include coke formation, sintering, and dealloying of the

bimetallic phase, all occur to some extent on alumina supported catalysts, resulting in their deactivation [5]. Coking and cracking side reactions happen via C-C bond activation and C-H bond overactivation at Lewis acid sites on the alumina surface that can be formed at high temperature in reducing conditions [27–29]. Commercially, on alumina supports, basic promoters such as Na, K, or Ca are commonly used to block sites that lead to coke formation at the cost of some catalytic activity [30]. Silica has been used recently since acid sites that may lead to coke formation are not present. In addition to being chemically inert, as we show in this study, silica provides a reservoir for coke species that appear to migrate away from the catalytically active metal nanoparticles, helping to maintain dehydrogenation activity for longer periods of time. The Pt-alloy catalysts in this work are supported on silica and one of the objectives of this study is to investigate the regenerability of silica-supported catalysts.

#### 2. Experimental Methods

#### Catalyst Synthesis

As a first step, the method of strong electrostatic adsorption method (SEA) was used on 5 g of commercially available silica (Sigma- Aldrich, Davisil grade 646) to prepare Zn/SiO<sub>2</sub>. Here, 0.68 g of Zn(NO<sub>3</sub>)<sub>2</sub>·6H<sub>2</sub>O (Sigma-Aldrich) was dissolved in 50 mL of deionized water (DI water) to obtain 3% Zn weight loading assuming all the Zn was loaded onto SiO<sub>2</sub>. Subsequently, ammonium hydroxide (NH<sub>4</sub>OH, Sigma-Aldrich) was added to a Zn(NO<sub>3</sub>)<sub>2</sub> solution to adjust the pH to 11–12. SiO<sub>2</sub> was added to the Zn solution and stirred for 10 min. The sample was vacuum filtered and washed with 50 mL of DI water three times. The wet powder was dried overnight at 125 °C and calcined at 300 °C for 3 h (10 °C/min). Pt was then added to Zn/SiO<sub>2</sub> by the pH adjusted incipient wetness impregnation method (IWI) to give 2% Pt weight loading in the final PtZn/SiO<sub>2</sub> catalyst. Its impregnation volume was calculated to be 1.16 mL/g by adding H<sub>2</sub>O dropwise to 1g of SiO<sub>2</sub> until it was saturated. Here, 0.2 g of Pt(NH<sub>3</sub>)<sub>4</sub>(NO<sub>3</sub>)<sub>2</sub> (Sigma-Aldrich) was dissolved in about 2 mL of DI water. Then, 1 mL of NH<sub>4</sub>OH was added to the Pt solution and stirred until all crystals dissolved. Water and NH<sub>4</sub>OH were added until the volume was sufficient to impregnate the pore volume of the SiO<sub>2</sub> and the pH of the Pt solution was between 11–12. The solution was added dropwise to the Zn/SiO<sub>2</sub> support while stirring. The catalyst was dried overnight at 125 °C, calcined at 200 °C for 3 hr (5 °C/min ramp), and reduced at 225 °C in 5% H<sub>2</sub>/N<sub>2</sub> at 100 cm<sup>3</sup>/min

for 30 min [15,31,32]. A similar approach was used to prepare PtMn and PtSn catalysts on silica. The weight loadings of the catalysts are as follows: PtZn/SiO<sub>2</sub> (2 wt% Pt, 3 wt% Zn), PtMn/SiO<sub>2</sub> (2 wt% Pt, 5 wt% Mn), PtSn/SiO<sub>2</sub> (2 wt% Pt, 1.5 wt% Sn). Alloy formation was confirmed by *in situ* XAS.

## Brunauer-Emmett-Teller (BET) Analysis

BET analysis of all samples was performed using a Micromeritics Gemini 2360 Surface Area Analyzer, using liquid nitrogen coolant, after a 24-hr degassing period at 120 °C under flowing nitrogen gas.

## X-ray Diffraction (XRD)

X-ray diffraction data was collected using a Rigaku SmartLab powder x-ray diffractometer, equipped with a Cu-target X-ray source (40 kV, 40 mA), a D/TeX Ultra 1-dimensional position sensitive detector, and a Ni-foil filter for reduction of the Cu-Kβ component of the diffracted radiation. Data was collected at 6° min<sup>-1</sup> from 3°-150° 2θ (0.02° step size). Lattice parameters were obtained via Rietveld refinement using the MDI Jade software package. Lattice parameters, crystallite size, and micro strain values were refined, as well as sample height error.

## Transmission Electron Microscopy (TEM)

Samples were dispersed in ethanol and mounted on holey carbon grids for examination the JEOL NeoARM 200CF transmission electron microscope equipped with a spherical aberration corrector to allow atomic resolution imaging and an Oxford Aztec Energy Dispersive System (EDS) for elemental analysis. The microscope is equipped with two large area JEOL EDS detectors for higher throughput in the acquisition of X-ray fluorescence signals. Images were recorded in annular dark field (ADF) mode and in annular bright field (ABF) mode.

## X-ray Absorption Spectroscopy (XAS)

In situ XAS experiments were performed at the MR-CAT 10-BM beamline at the Argonne APS and the 8-ID ISS beamline at the Brookhaven NSLS-II [33]. The catalyst materials were scanned at the Pt L<sub>3</sub> edge (11.564 keV) for the PtSn/SiO<sub>2</sub>, PtMn/SiO<sub>2</sub>, and PtZn/SiO<sub>2</sub> samples. Samples were ground to a fine powder and packed into a sample holder. The sample holder was

placed in an *in situ* cell in the middle of a quartz tube with leak-tight end caps containing X-ray-transparent Kapton windows. All the samples were placed into the same cell for simultaneous analysis. The samples were reduced in 5% H<sub>2</sub>/He at 550 °C for 30 minutes, then cooled to 25 °C in He and scanned. Sample measurement was accompanied by a Pt foil scan, used for energy calibration, which was obtained simultaneously using a third ion chamber. The X-ray absorption near edge structure (XANES) spectra were used to identify the oxidation state while the extended X-ray absorption fine structure (EXAFS) provided information about the number, identity, and distance of local scattering atoms. XANES and EXAFS data were obtained and interpreted using WinXAS v 4.0 software.[34] Feff6 calculations were performed using a single scattering atom of each type placed at a certain distance from a main Pt atom. [35] The type of atom and distance is as follows: Pt–Zn = 2.66 Å, Pt–Pt = 2.77 Å, Pt–Mn = 2.66 Å, Pt–Sn = 2.81 Å, Pt–O = 2.05 Å. The standard EXAFS fit was performed on the reduced (metallic) sample.

#### Reaction Testing

Reaction conditions are defined throughout the results section because of the variety of conditions used. The most common conditions, however, are termed as "coking conditions" and "lower-coking conditions". Coking conditions indicates 5% propane in balance Ar at 550 °C while lower-coking conditions indicates H<sub>2</sub> cofeeding in ratios that are typically 1:1 or 2:1 with respect to propane at 550 °C or 600°C.

#### Results

Table 1 provides a summary of the XAS characterization of the Pt alloy catalysts prepared for this study. The samples were reduced in 5% H<sub>2</sub>/He at 550 °C for 30 minutes before performing the spectroscopy in transmission mode. Figures S1 and S2 show the XANES and the EXAFS for the Pt alloy catalysts, respectively. The XANES energy, defined as the inflection point of the initial photoexcitation, increased with alloy formation by 0.5 to 0.7 eV, listed in Table 1, compared to the Pt foil. This shift is consistent with alloy formation. Figure S2 contains the EXAFS spectra, which all show a noticeable difference in magnitude and peak position compared to the Pt foil used as a reference, which has three peaks. This suggests scattering paths other than Pt-Pt, and the small magnitude may be attributed to destructive interference between the scattering paths. Upon fitting, the PtZn/silica sample had Pt-Zn scattering path was present at a bond distance longer than the Pt-

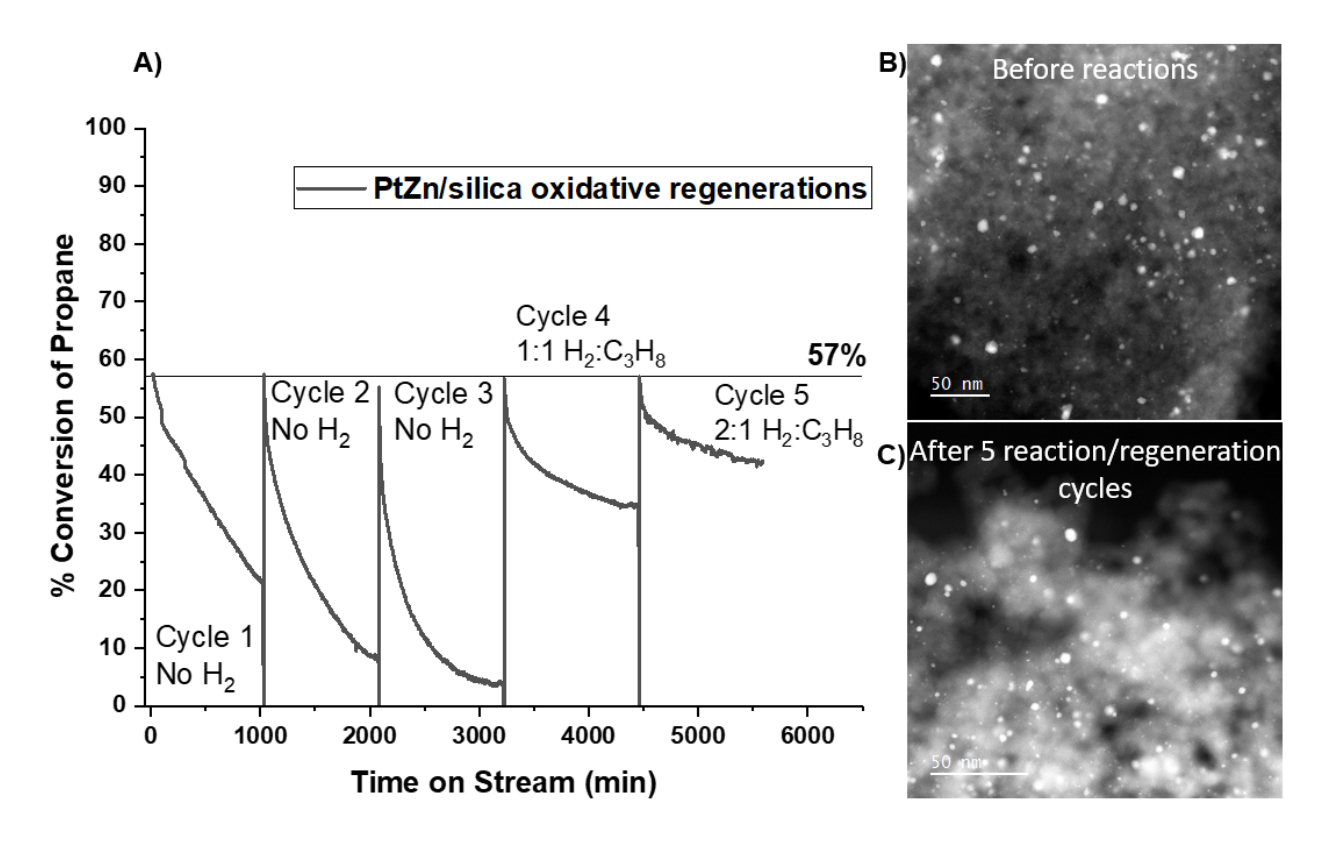
Pt scattering path, which is typical of a Pt<sub>1</sub>Zn<sub>1</sub> structure previously reported [11]. The ratio of Pt-Pt bonds to Pt-Zn bonds is roughly 3:1, suggesting the formation of Pt-rich nanoparticles, i.e., a Pt core and surface Pt<sub>1</sub>Zn<sub>1</sub> surface. For the PtMn/silica catalyst, the Pt-Pt:Pt-Mn coordination ratio is roughly 2:1, and the bond distance is the same between both scattering paths at a bond distance slightly shorter than that of Pt-Pt [20]. This suggests the formation of full-phase Pt<sub>3</sub>Mn nanoparticles. Similarly, for the PtSn/silica sample, the Pt-Pt:Pt-Sn coordination ratio is roughly 2:1, and the bond distance is longer than that of Pt-Pt, suggesting the formation of full-phase Pt<sub>3</sub>Sn nanoparticles. This phase and bond distance extension is confirmed using XRD, as shown in Figure S3.

Table 1. Pt L<sub>3</sub> Edge EXAFS fits for the PtZn/silica, PtMn/silica, and PtSn/silica samples.

Sample	Edge energy	Scattering	CN	R	$\Delta \sigma^2 (\mathring{A}^2)$	Shift in E <sub>o</sub>
	(keV)	Pair	$(\pm 10\%)$	$(\pm 0.02~\text{Å})$		(eV)
Pt foil	11.5640	Pt-Pt	12.0	2.77	-	7.5
re-2Pt-3Zn	11.5647	Pt-Pt	6.1	2.72	0.005	3.5
		Pt-Zn	1.7	2.81	0.005	4.5
re-2Pt-5Mn	11.5645	Pt-Pt	5.7	2.68	0.004	2.3
		Pt-Mn	2.1	2.69	0.004	2.6
re-2Pt-1.5Sn	11.5647	Pt-Pt	5.4	2.77	0.004	1.3
		Pt-Sn	2.4	2.79	0.004	1.8

Figure 1A shows the propane dehydrogenation reactivity of the Pt-Zn catalyst for 5 cycles involving  $\sim$ 1000 minutes of reaction. After each reaction cycle, an oxidative regeneration was performed with air at 420°C for 1 hour. The role of added hydrogen (H<sub>2</sub>:C<sub>3</sub>H<sub>8</sub> = 0,1, or 2) on the deactivation rate was studied for propane dehydrogenation (10% propane in Ar) on the PtZn/SiO<sub>2</sub> catalyst using a WHSV of 11.4 g propane/g catalyst/hr at 550°C. As seen in Figure 1A, without added hydrogen, the catalyst deactivates rapidly during cycles 1, 2, and 3. The figure reports conversion for each reaction cycle ( $\sim$ 18 hours). Since the catalyst regains its initial conversion at the beginning of each cycle, this suggests that the catalyst can be regenerated using oxidative regeneration without sintering of the alloy NPs. Cycle 4 and Cycle 5 involve co-feeding hydrogen in a ratio of H<sub>2</sub>:C<sub>3</sub>H<sub>8</sub> = 1 and 2 respectively. Figure 1A shows the extent of single-cycle deactivation during cycles 4 and 5 was much less pronounced than cycles 1-3. Cycle 5 provided stable operation, achieving 84% of equilibrium conversion at the end of the 20-hour run. By

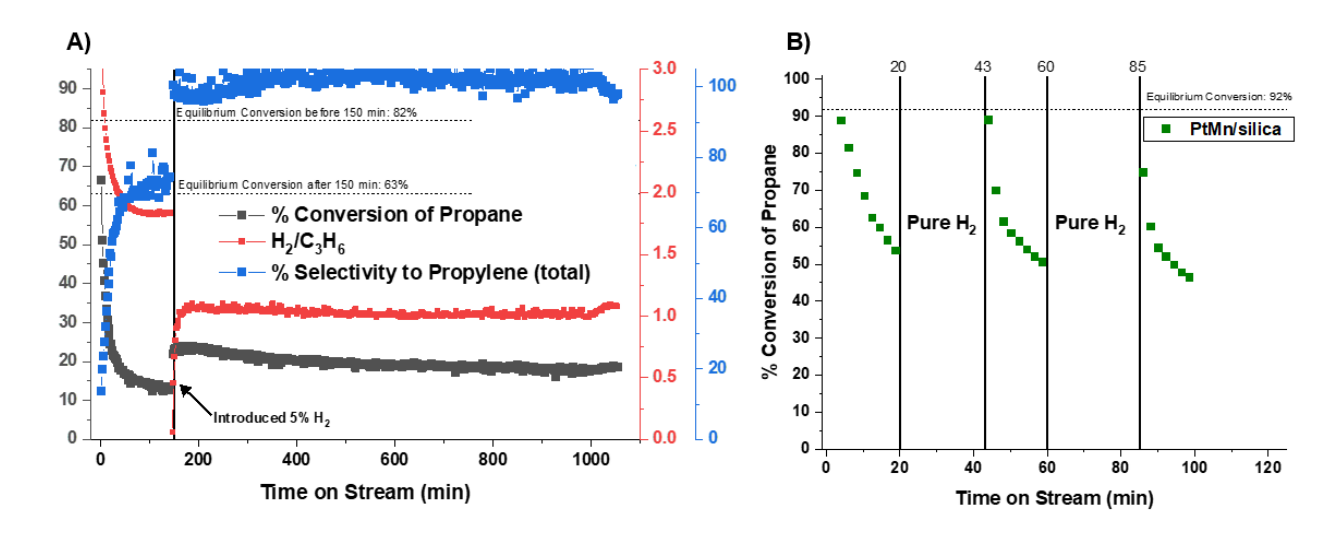
contrast, in cycles 1-3 with no added hydrogen, the catalyst achieved about 25% of equilibrium conversion at the end of ~ 20 hours of operation. These results demonstrate that co-feeding hydrogen improves catalyst stability and achieves operation closer to equilibrium. After 5 cycles, the catalyst was removed from the reactor for examination by electron microscopy. The HAADF STEM images in Figure 1B show that the catalyst particle size distribution remains, within experimental error, unchanged after 5 reaction/oxidation/re-reduction cycles, indicating that sintering may not be the primary deactivation mechanism and that the silica supported PtZn catalyst can be oxidatively regenerated without causing sintering of the NPs. The initial composition by SEM/EDS is 2.3% Pt and 3.2% Zn, by weight, as seen in Figure S4. Figure S5 contains a similar plot demonstrating the regenerability of PtSn/silica in air.



**Figure 1.** A) % Conversion as a function of time on stream for PtZn/silica in three sets of conditions: (1) 10% propane in Ar (cycles 1-3), (2) 10% propane and 10% H<sub>2</sub> in Ar (cycle 4), and (3) 10% propane and 20% H<sub>2</sub> in Ar (cycle 5). The reaction was carried out isothermally at 550°C. At the end of each run (except the last), the catalyst was regenerated in air (40mL/min) at 420°C for 1 hr. B) HAADF STEM image of "as prepared" PtZn/silica pre-treated in H<sub>2</sub>. C) HAADF

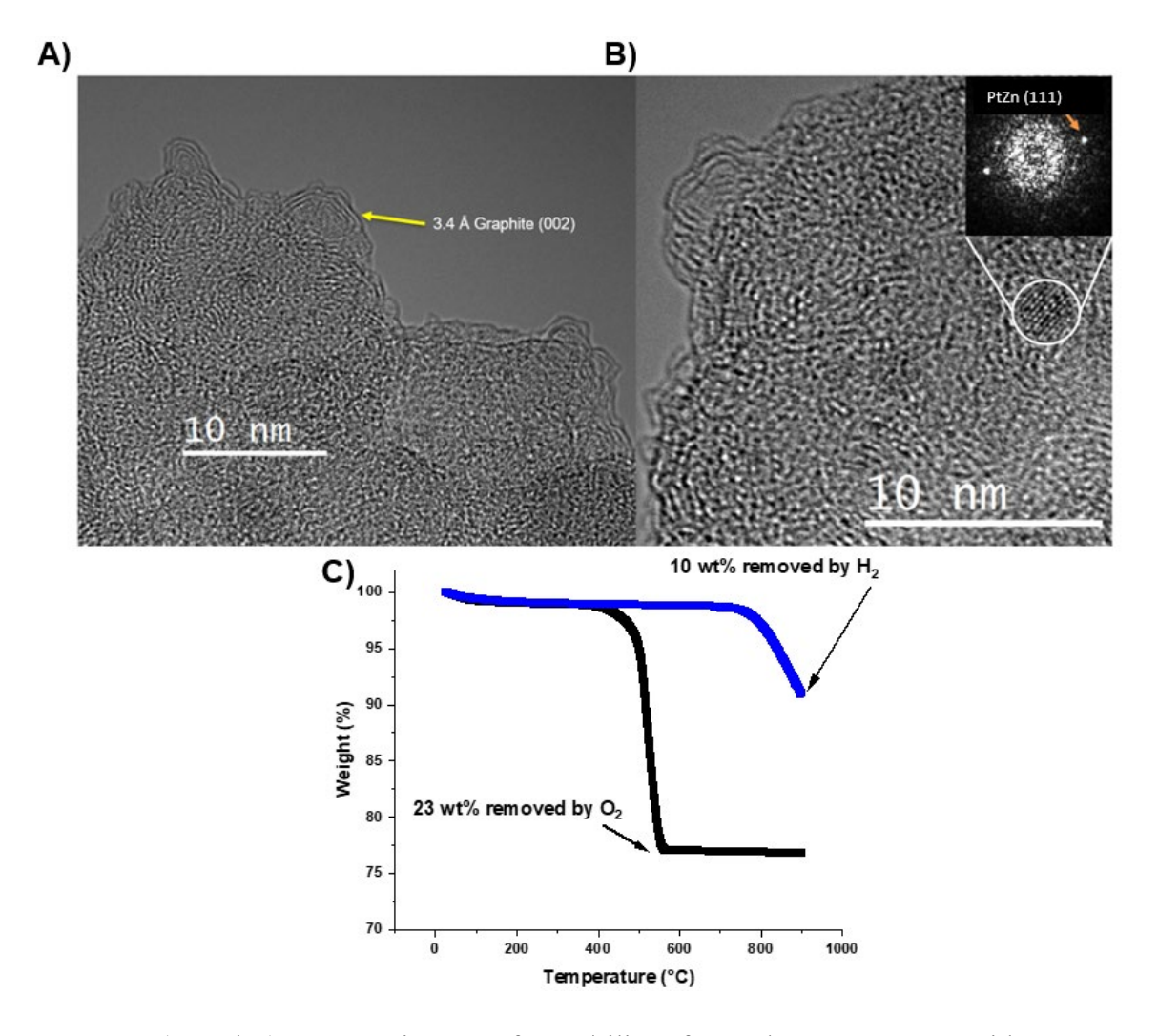
STEM image of PtZn/silica after five 18-hr cycles followed by 1 hr regenerations using air at 420°C (after cycle 5 without regeneration).

Next, we explored whether the deactivation could be recovered by *in-situ* addition of H<sub>2</sub> to the feed after the catalyst had partially deactivated. A stream of 5% propane in Ar (40mL/min total flow) was used for PDH using PtMn/SiO<sub>2</sub> (2%Pt 5%Mn) at 550 °C. When H<sub>2</sub> was introduced after 150 minutes on stream in a ratio of H<sub>2</sub>:C<sub>3</sub>H<sub>8</sub> = 1, as shown in Figure 2A, the conversion increased with an accompanying shift in overall stability. In Figure S6, a similar experiment was run with earlier introduction of H<sub>2</sub> at 60 minutes on stream. A greater fraction of the initial activity could be recovered by starting the H<sub>2</sub> treatment at shorter times on stream. Figure 2A also provides the conversion versus time, final conversions, and equilibrium conversions for the initial part of the run, without added H<sub>2</sub>. Conversion and selectivity are defined in Equations S1-S3. The contrast between the "coking" conditions, for example, without H<sub>2</sub> and the "lower-coking conditions", i.e., co-fed H<sub>2</sub> is dramatic in terms of selectivity; we achieve conversions that are closer to equilibrium upon the addition of cofed hydrogen, in which is consistent with the literature [8]. Figure 2B depicts a "pulsing" experiment with PtMn/silica which entails alternating periods of 20 min on stream in coking conditions (40 mL/min of 5% propane in Ar) and 20 min with pure H<sub>2</sub> flow (40mL/min). 20 minute "pulses" were chosen based on the data in Figure S7 (in the SI) suggesting that at earlier times on stream, a greater effect can be obtained with H<sub>2</sub>. Under these reaction conditions, the high activity, the gas phase selectivity and total selectivity are similar to those seen on the fresh catalyst. During the H<sub>2</sub> regeneration process, no gas phase products are observed via MicroGC, suggesting either that the amounts of carbon deposited on the NPs are too small to be detected or that the coke cannot be reacted away in H<sub>2</sub> presumably because most of it is located on the support [36]...



**Figure 2.** A) % Conversion of propane (black), % propylene selectivity (blue), and H<sub>2</sub>/C<sub>3</sub>H<sub>6</sub> (red) as a function of time on stream for 60 mg of PtMn/silica. The reaction was carried out isothermally at 550°C. The feed is initially 5% propane in Ar with a total flow rate of 40 mL/min. At a time on stream of 150 min, 5% H<sub>2</sub> was introduced, making the feed 5% propane, 5% H<sub>2</sub>, and 90% Ar with a total flowrate of 40 mL/min. B) % Conversion vs time on stream for 60 mg of PtMn/silica. Reaction cycles (green squares) of 20 mins on stream with 5% propane in N<sub>2</sub> and 20 mins with pure H<sub>2</sub> flowing over the catalyst with a total flow rate of 40 mL/min. The reaction and H<sub>2</sub> pulsing were carried out isothermally at 600°C.

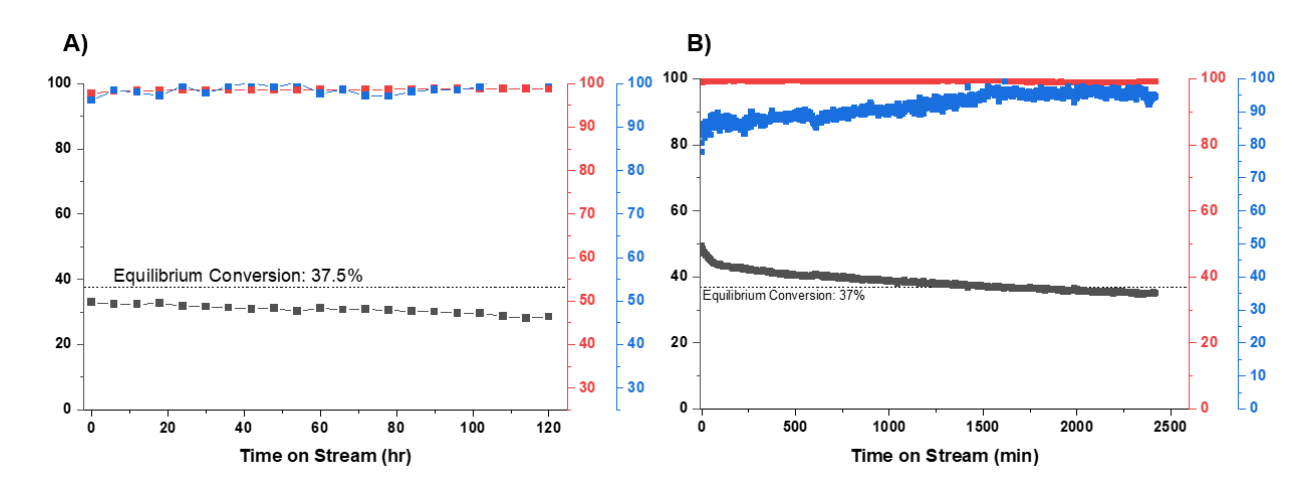
To further investigate the nature of the coke on a fully deactivated catalyst, 60 mg of PtZn/silica catalyst was run for 40 hours on stream with 5% propane in argon (40mL/min total flow rate) which we define as coking conditions. In Figure 4, HRTEM images and the TGA profile of the spent PtZn/silica catalyst that has nearly completely deactivated by coking are shown. Figure 4 shows that multi-layer graphitic carbon is present all over the support and possibly on the nanoparticles. However, the surface of the nanoparticles cannot be directly imaged because of overlap with the silica support. Previous work done by Pham et al. [37,38] reported images of monolayers of carbon on silica supports, and comparing with those images it becomes clear that we have multilayer carbon on this sample based on the crystalline lattice fringes at the edge of the silica that can be indexed to the graphite (002) planes. This multilayer carbon comprises about 23 wt % of the entire sample (PtZn/silica) based on TGA measurement in air. Redekop et al. (ref) describe a similar situation with multilayer crystalline carbon that forms all over the catalyst and catalyst support, on Pt/Mg(Al)O<sub>x</sub>.



**Figure 3.** (A and B) HRTEM images of PtZn/silica after 40 hours on stream with a 5% propane in Ar feed. (C) TGA profile of this deactivated PtZn/silica catalyst when heated in air (black) and 4% H<sub>2</sub> in N<sub>2</sub> (blue).

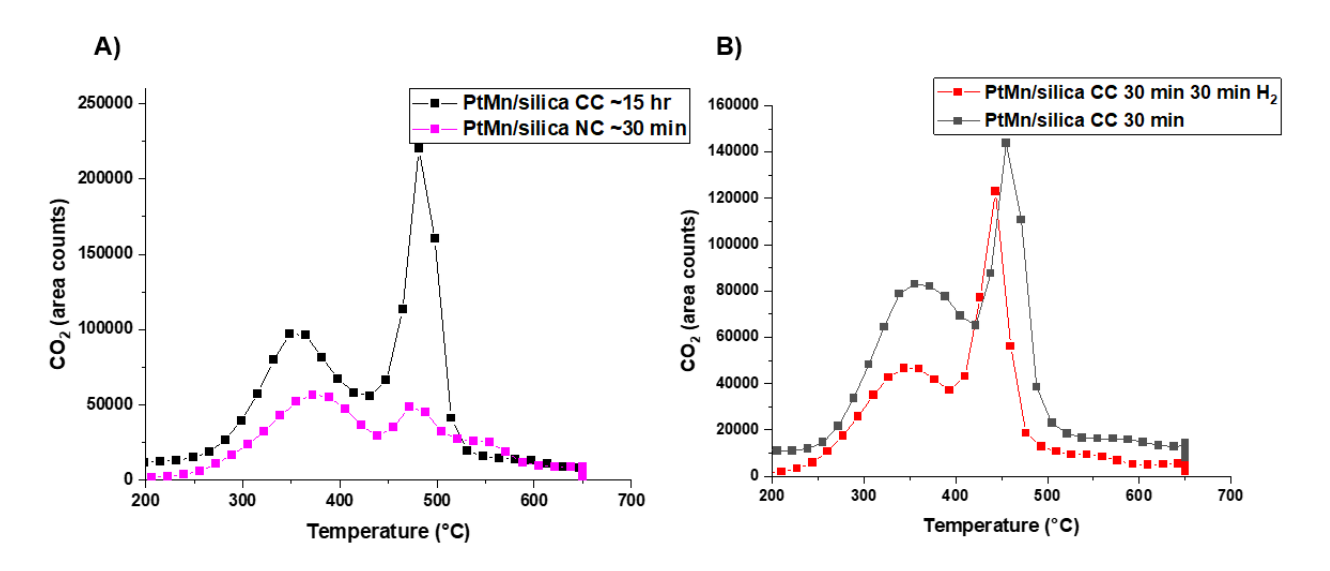
Having established the role of cofed H<sub>2</sub> on the PtMn and PtZn catalysts, conditions that would lead to longer lifetimes were investigated. Figure 4A depicts the % conversion, % gas phase selectivity, and % total selectivity for 250 mg PtSn/silica at 600°C for 5 days on stream operating initially at 97% of equilibrium conversion, dropping (after 120 hr) to 77% of equilibrium for this set of conditions. The total flow is 100mL/min, and the feed concentration is 55% propane 40% H<sub>2</sub> and 5% N<sub>2</sub>. The fact that the total selectivity and the gas phase selectivity are similar suggests there is minimum coking or cracking side reactions under these operating conditions. It was found that, in the presence of enough H<sub>2</sub>, the PtSn/silica catalyst effectively avoids both cracking and coking side reactions, leading to exceptionally good stability (at close to equilibrium conversion).

Figure 4B shows that the PtMn catalyst shows similar stable long-term performance in the presence of co-fed H<sub>2</sub>.



**Figure 4.** % Conversion (black), % Gas phase selectivity (red), and % total selectivity (blue) as a function of time on stream for A) 250 mg of PtSn/silica at 600°C in 55% propane 5% N<sub>2</sub> and 45% H<sub>2</sub>. B) 60 mg PtMn/silica at 600 °C (furnace set point) in 45% propane 45% H<sub>2</sub> and 10% H<sub>2</sub>.

To explore whether the coke migration from the Pt alloy NPs onto the SiO<sub>2</sub> support was responsible for the stability observed with cofed H<sub>2</sub>, in situ temperature programmed oxidations (TPO) were performed. After the reaction, the catalyst is cooled to 40°C, purged with N<sub>2</sub>, and then reacted in situ with 40mL/min of 10% O<sub>2</sub> in N<sub>2</sub>; while, the furnace ramped to 650°C at 10°C/min. Figure 5 shows the TPO profiles for PtMn/silica catalysts that have seen a 0:1 and 1:1 H<sub>2</sub>:C<sub>3</sub>H<sub>8</sub> feed ratios for different amounts of time and reaction conditions (coking versus non-coking). Figure 5a shows that coking conditions for 15 hours result in the largest amount of coke that is also the most difficult to remove, judging by the higher temperature required to fully oxidize the coke. There appear to be two types of coke, one which is oxidized at low temperature, about 350 °C, and one at higher temperature, which is oxidized at about 450 °C. Coking for 30 minutes results in the formation of less coke, which can also be removed at a lower temperature. Under non-coking conditions, which includes co-feeding H<sub>2</sub> for 30 minutes, we see the least amount of coke deposited. Both the low temperature coke, as well as the high temperature coke is reduced as seen from the pink verse the blue curves in Figure 5a. Figure 5b illustrates that an additional H<sub>2</sub> treatment for 30 minutes after use in coking reaction conditions for 30 minutes results in the removal of some coke, and the coke that remains is more easily removed by oxidation.



**Figure 5.** A) TPO profile of a PtMn/silica catalyst after 15 hr in coking conditions (5% propane in Ar) at 550°C, cooled in the reaction atmosphere, purged with nitrogen at room temperature, and then exposed to 40mL/min of 10% O<sub>2</sub> in N<sub>2</sub> by heating at 10°C/min to 650°C and then held for 30 min. The same procedure was performed for separate PtMn/silica samples (60mg) that had seen coking conditions for 30 min and non-coking conditions (45% propane 45% H<sub>2</sub> & 10% N<sub>2</sub>) for 30 min. B) Direct comparison of the coke deposited on PtMn/silica after coking conditions for 30 min with andwithout an additional 30 min H<sub>2</sub> treatment (also cooled in H<sub>2</sub> instead of reaction conditions).

# 3. Discussion

Figure 1 shows that the PtZn/silica catalyst can be oxidatively regenerated via treatment in air at 420°C for at least one hour. The loss of activity becomes more rapid with each successive reaction cycle, suggesting that the regenerated catalyst was different from the initial catalyst. With each new reaction cycle, coke accumulation is seen to occur more rapidly perhaps due to the residual coke left after incomplete burn-off. The residual coke may cause more facile nucleation and growth of freshly deposited coke. The reactions in Figure 1 were run in 40mL/min of 10% propane in inert, but at lower partial pressures of propane, deactivation is even more pronounced because experiments at 5% propane in Ar show even more precipitous drops in conversion as a function of time. Despite incomplete removal of coke species, the catalyst can be restored to its initial conversion and can even operate in a stable fashion with co-fed H<sub>2</sub>, as is shown in cycle 4 and 5. The STEM image of the catalyst in Figure 1 showed no increase in particle size after the

reaction cycles, suggesting that silica supported catalysts can be successfully regenerated by oxidation at low temperature.

A study of this reaction with temporal analysis of products (TAP) [14] had elucidated many of the phenomena on a Pt/Mg(Al)O<sub>x</sub> catalyst that we also see with Pt alloys on silica. It was concluded that the most active sites are rapidly covered by coke in the initial exposure of the catalyst to propane. It was concluded that graphene-like layers are formed on and near the catalyst support and that the TPO profiles can be interpreted in terms of coke being present on the metal and coke on the support [14]. When the reactants are passed over the catalyst in pulses, alternating with an inert gas, a modest increase in propylene production was observed for a short period of time. This increase in conversion is attributed to an additional transport process whereby coke precursors migrate away from the catalyst NPs. The increase in activity, by means of time on stream in inert, is short lived and not useful from an operational perspective. In this work, we show that the transport process that allows coke to migrate away from the surface is accelerated in the presence of pure H<sub>2</sub> and that this can be used as a regeneration strategy to stave off the need for oxidative regeneration.

Figure 2A shows that for a coke-deactivated catalyst, addition of H<sub>2</sub> to the feed stream, not only leads to a sudden increase in the conversion, but also to a much slower deactivation rate. Thus, H<sub>2</sub> not only leads to the recovery of active sites but slows the deactivation rate upon its continuous feeding thereafter. This closer approach to equilibrium for both ethane and propane has been reported in the literature [7,8]. However, the spontaneous recovery of the catalyst activity and selectivity of a coked catalyst accelerated in the presence of H<sub>2</sub> has not been reported in the literature on silica-supported catalysts. Figure 2B shows that if a catalyst is coked for a shorter time, nearly complete recovery of the initial conversion can be restored. Similar observations were reported in a TAP reactor study describing pulsing in reactant and then waiting at reaction temperature for the next pulse, but the recovery in performance was not very significant from an applied perspective [14]. There is also a comparative study detailing similar regeneration treatments of H<sub>2</sub> and N<sub>2</sub> as a regeneration strategy for a PtSn/alumina catalyst and come to the conclusions that the mobility of coke is "activated" in the presence of H<sub>2</sub> [39]. In this work, we show that initial activity can be recovered using H<sub>2</sub> alone if done early and frequently enough on silica supported Pt alloys. It can be seen, from Figure S12, that regeneration in N<sub>2</sub> at the reaction

temperature allows one to operate at the same conversion because of a similar mechanism, coke mobility from NP to support, except that coke mobility is not as pronounced, since it is not "activated" like it is in the presence of H<sub>2</sub>.

As shown in Figure 3 for a PtZn/silica catalyst that was highly deactivated, we observe graphitic carbon (identified from the lattice fringes) in all regions of the catalyst, on both the metal and the support. TGA in flowing air shows a weight loss indicating about 23 wt.% of coke had accumulated on the catalyst. For the same sample, TGA in H<sub>2</sub> surprisingly indicated that slightly less than half the coke could be removed as compared to the TGA done in air. It should be noted that a non-zero amount of weight loss is observed in TGA (dilute H<sub>2</sub>) at reaction conditions suggesting there is some degree of coke hydrogenation that is difficult to detect. Attempts to characterize the species that may be reacting via hydrogenation via TPR-MS or by MicroGC analysis are inconclusive. However, the TGA done in dilute H<sub>2</sub> suggests some coke species may be liberated by hydrogenation depending on the type and location of said coke. This observation is something also evidenced by the in situ TPO data discussed later in this discussion.

Figure 4 demonstrates the stability one can achieve with cofeeding H<sub>2</sub> in large enough amounts (~1:1 with propane). The mechanistic aspects of mitigating coke deactivation (suppression) by cofeeding hydrogen for propane dehydrogenation have been well established. Saerens et al [7] proposed that H<sub>2</sub> competes with coke precursors (i.e., CCH<sub>3</sub> ethylidyne and CH methylidyne) for active sites, decreases the adsorption strength of propylene, and increases the energy barrier for coke producing side reactions. This explanation seems to agree with the findings from Figure 1, which illustrates the stabilization of the catalyst with co-fed H<sub>2</sub>, but it should be noted that H<sub>2</sub> does not completely prevent coking, and coke mobility/location may also play a significant role in catalyst stability. Eventually, all catalysts deposit enough coke to lead to a loss of conversion and require regeneration to restore activity. Therefore, the regenerability of the catalyst is paramount to successful implementation in industrial processes.

In Figure 5, temperature programed oxidation of the coke shows that there are two types of coke, which oxidize at different temperatures. Since Pt is a highly effective oxidation catalyst, it is likely that the low temperature coke is on or near the Pt alloy NPs, while the coke which is oxidized at higher temperature must lie on the support. In Figure 5A, for a PtMn catalyst run in

propane alone for 30 min and 15 h, the amount of coke on the alloy NPs is very similar, while there is much more coke on the support when reacted for a longer reaction time. Although longer reaction times lead to more coke on the support, the increase is not linearly proportional with reaction time. Approximately as much coke is deposited in the first 30 min as the next 14+ hours. Thus, coke deposition on the metal NPs is rapid and doesn't change much at longer times, while the coke on the support deposits quickly during the first few minutes and more slowly at longer times. Treatment of this catalyst in H<sub>2</sub>, Figure 5B, suggests that a significant amount of coke on the metal NP is removed, which is consistent with an increase in conversion observed in Figures 2 and 5. The amount of coke on the support, i.e., the high temperature coke, however, is little changed, see Figure 5A (blue and red squares, 30 min with and without H<sub>2</sub>) and Figure 5B. Thus, once the coke on the support has formed, it is not readily removed by H<sub>2</sub>.

While Figure 2B shows that for short reaction times, the initial activity can be restored by H<sub>2</sub> regeneration, the TPO in Figure 5 suggests this is not a viable approach after a long-term reaction. This is because while H<sub>2</sub> regeneration will remove coke from the metallic NPs, it is not able to remove coke from the support, which will build up with long times on stream and eventually deactivate the catalyst necessitating oxidative regeneration. A more effective strategy may be to co-feed propane and H<sub>2</sub> to limit the amount of coke on the metal NP and support and mitigate the deactivation obtaining longer on-stream operation, as seen in Figure S13. Low temperature oxidation effectively removes the carbon from the metallic NPs, but longer (oxidative) regeneration times or higher temperature are required to remove coke from the support. By cofeeding propane and H<sub>2</sub>, the amount of coke on the support can be suppressed, thus, low temperature oxidation will be effective at removing all the coke and restoring the catalyst performance. The low temperature regeneration will also lead to long-term operation since the NPs do not sinter at these lower temperatures. With low coke on catalysts, it is also possible to use higher oxygen concentrations since the oxidation exotherms will be much less pronounced.

#### 4. Conclusions

The addition of H<sub>2</sub> has a clear stabilizing effect on silica supported Pt alloys in PDH consistent with the established literature. In the absence of co-fed H<sub>2</sub>, propane dehydrogenation leads to rapid coking of the metallic NPs and the silica support. Coke formation on the metallic NPs occurs in

the first 30 min with little additional coke at longer reaction times. Coking on the support also occurs rapidly during the first 30 min but continues to increase with increasing reaction time. Complete loss of conversion leads to coke levels of about 25%. Oxidation at 420 °C does not sinter the metallic NPs and restores the initial conversion; however, with each successive reaction cycle, the deactivation rate become more rapid suggesting that not all the coke has been removed from the catalyst. Treatment with H<sub>2</sub> or co-feeding H<sub>2</sub> partially or fully restores coke deactivated catalysts if applied after short reaction cycles. Co-fed H<sub>2</sub> lowers the overall deactivation rate while allowing closer approach to equilibrium and higher conversion. Analysis of the coked catalysts suggests there are two types of coke, i.e., on the metal NPs and on the support though the reactivity of the coke and support appears to be very different Treatment in H<sub>2</sub> lowers the coke on the metal NPs but does not reduce the amount of coke present on the support. High partial pressures of cofed H<sub>2</sub>, however, are effective at significantly lowering the amount of coke on the support. Thus, by co-feeding H<sub>2</sub> and propane, lower deactivation is achieved, and longer reaction cycles are possible. Maintaining low coke amounts on the support allows low temperature oxidative regeneration to effectively remove all the coke from the catalyst, restoring the initial activity for long-term performance.

## 5. Acknowledgements

This work was supported by NSF/ERC CISTAR, which is supported by the National Science Foundation under Cooperative Agreement No. EEC-164772. Acquisition of the TEM was supported by the NSF MRI Grant DMR-1828731. The research used resources at the 8-ID beamline of the National Synchrotron Light Source II, a US Department of Energy Office of Science User Facility operated by Brookhaven National Laboratory under contract no. DE-SC0012704. Use of the Advanced Photon Source, a US Department of Energy Office of Basic Energy Sciences, was supported under contract no. DE-AC02-06CH11357. The MRCAT beamline 10-BM is supported by the Department of Energy as well as the MRCAT member institutions.

#### References

- [1] U.S. Energy Information Administration. Annual Energy Outlook 2022; U.S. Energy Information Administration: 2022.
- [2] E. National Academies of Sciences, The Changing Landscape of Hydrocarbon Feedstocks for Chemical Production: Implications for Catalysis: Proceedings of a Workshop, 2016. https://doi.org/10.17226/23555.
- [3] J.J.H.B. Sattler, J. Ruiz-Martinez, E. Santillan-Jimenez, B.M. Weckhuysen, Catalytic Dehydrogenation of Light Alkanes on Metals and Metal Oxides, Chem. Rev. 114 (2014) 10613–10653. https://doi.org/10.1021/cr5002436.
- [4] S. Chen, X. Chang, G. Sun, T. Zhang, Y. Xu, Y. Wang, C. Pei, J. Gong, Propane dehydrogenation: catalyst development, new chemistry, and emerging technologies, Chem. Soc. Rev. 50 (2021) 3315–3354. https://doi.org/10.1039/D0CS00814A.
- [5] H.N. Pham, J.J.H.B. Sattler, B.M. Weckhuysen, A.K. Datye, Role of Sn in the Regeneration of Pt/γ-Al2O3 Light Alkane Dehydrogenation Catalysts, ACS Catal. 6 (2016) 2257–2264. https://doi.org/10.1021/acscatal.5b02917.
- [6] Shaping the future of on-purpose propylene production, (n.d.). https://www.hydrocarbonprocessing.com/magazine/2017/april-2017/special-focus-petrochemical-developments/shaping-the-future-of-on-purpose-propylene-production (accessed December 19, 2022).
- [7] S. Saerens, M.K. Sabbe, V.V. Galvita, E.A. Redekop, M.-F. Reyniers, G.B. Marin, The Positive Role of Hydrogen on the Dehydrogenation of Propane on Pt(111), ACS Catal. 7 (2017) 7495–7508. https://doi.org/10.1021/acscatal.7b01584.
- [8] G. Siddiqi, P. Sun, V. Galvita, A.T. Bell, Catalyst performance of novel Pt/Mg(Ga)(Al)O catalysts for alkane dehydrogenation, J. Catal. 274 (2010) 200–206. https://doi.org/10.1016/j.jcat.2010.06.016.
- [9] D. Akporiaye, S.F. Jensen, U. Olsbye, F. Rohr, E. Rytter, M. Rønnekleiv, A.I. Spjelkavik, A Novel, Highly Efficient Catalyst for Propane Dehydrogenation, Ind. Eng. Chem. Res. 40 (2001) 4741–4748. https://doi.org/10.1021/ie010299+.
- [10] V. Galvita, G. Siddiqi, P. Sun, A.T. Bell, Ethane dehydrogenation on Pt/Mg(Al)O and PtSn/Mg(Al)O catalysts, J. Catal. 271 (2010) 209–219. https://doi.org/10.1016/j.jcat.2010.01.016.
- [11]P. Sun, G. Siddiqi, M. Chi, A.T. Bell, Synthesis and characterization of a new catalyst Pt/Mg(Ga)(Al)O for alkane dehydrogenation, J. Catal. 274 (2010) 192–199. https://doi.org/10.1016/j.jcat.2010.06.017.
- [12] J. Wu, Z. Peng, A.T. Bell, Effects of composition and metal particle size on ethane dehydrogenation over PtxSn100−x/Mg(Al)O (70≤x≤100), J. Catal. 311 (2014) 161–168. https://doi.org/10.1016/j.jcat.2013.11.017.
- [13] J. Wu, S. Mallikarjun Sharada, C. Ho, A.W. Hauser, M. Head-Gordon, A.T. Bell, Ethane and propane dehydrogenation over PtIr/Mg(Al)O, Appl. Catal. Gen. 506 (2015) 25–32. https://doi.org/10.1016/j.apcata.2015.08.029.
- [14] E.A. Redekop, S. Saerens, V.V. Galvita, I.P. González, M. Sabbe, V. Bliznuk, M.-F. Reyniers, G.B. Marin, Early stages in the formation and burning of graphene on a Pt/Mg(Al)Ox dehydrogenation catalyst: A temperature- and time-resolved study, J. Catal. 344 (2016) 482–495. https://doi.org/10.1016/j.jcat.2016.10.023.
- [15] C.-W. Chang, H.N. Pham, R. Alcala, A.K. Datye, J.T. Miller, Dehydroaromatization Pathway of Propane on PtZn/SiO2 + ZSM-5 Bifunctional Catalyst, ACS Sustain. Chem. Eng. 10 (2022) 394–409. https://doi.org/10.1021/acssuschemeng.1c06579.
- [16] H. Xiong, S. Lin, J. Goetze, P. Pletcher, H. Guo, L. Kovarik, K. Artyushkova, B.M. Weckhuysen, A.K. Datye, Thermally Stable and Regenerable Platinum—Tin Clusters for Propane Dehydrogenation Prepared by Atom Trapping on Ceria, Angew. Chem. 129 (2017) 9114—9119. https://doi.org/10.1002/ange.201701115.

- [17]S. Chen, Z.-J. Zhao, R. Mu, X. Chang, J. Luo, S.C. Purdy, A.J. Kropf, G. Sun, C. Pei, J.T. Miller, X. Zhou, E. Vovk, Y. Yang, J. Gong, Propane Dehydrogenation on Single-Site [PtZn4] Intermetallic Catalysts, Chem. 7 (2021) 387–405. https://doi.org/10.1016/j.chempr.2020.10.008.
- [18] E.C. Wegener, B.C. Bukowski, D. Yang, Z. Wu, A.J. Kropf, W.N. Delgass, J. Greeley, G. Zhang, J.T. Miller, Intermetallic Compounds as an Alternative to Single-atom Alloy Catalysts: Geometric and Electronic Structures from Advanced X-ray Spectroscopies and Computational Studies, ChemCatChem. 12 (2020) 1325–1333. https://doi.org/10.1002/cctc.201901869.
- [19] V.J. Cybulskis, B.C. Bukowski, H.-T. Tseng, J.R. Gallagher, Z. Wu, E. Wegener, A.J. Kropf, B. Ravel, F.H. Ribeiro, J. Greeley, J.T. Miller, Zinc Promotion of Platinum for Catalytic Light Alkane Dehydrogenation: Insights into Geometric and Electronic Effects, ACS Catal. 7 (2017) 4173–4181. https://doi.org/10.1021/acscatal.6b03603.
- [20] Z. Wu, B.C. Bukowski, Z. Li, C. Milligan, L. Zhou, T. Ma, Y. Wu, Y. Ren, F.H. Ribeiro, W.N. Delgass, J. Greeley, G. Zhang, J.T. Miller, Changes in Catalytic and Adsorptive Properties of 2 nm Pt3Mn Nanoparticles by Subsurface Atoms, J. Am. Chem. Soc. 140 (2018) 14870–14877. https://doi.org/10.1021/jacs.8b08162.
- [21] A.H. Motagamwala, R. Almallahi, J. Wortman, V.O. Igenegbai, S. Linic, Stable and selective catalysts for propane dehydrogenation operating at thermodynamic limit, Science. 373 (2021) 217–222. https://doi.org/10.1126/science.abg7894.
- [22] N.M. Schweitzer, B. Hu, U. Das, H. Kim, J. Greeley, L.A. Curtiss, P.C. Stair, J.T. Miller, A.S. Hock, Propylene Hydrogenation and Propane Dehydrogenation by a Single-Site Zn2+ on Silica Catalyst, ACS Catal. 4 (2014) 1091–1098. https://doi.org/10.1021/cs401116p.
- [23]B. Hu, N.M. Schweitzer, G. Zhang, S.J. Kraft, D.J. Childers, M.P. Lanci, J.T. Miller, A.S. Hock, Isolated FeII on Silica As a Selective Propane Dehydrogenation Catalyst, ACS Catal. 5 (2015) 3494–3503. https://doi.org/10.1021/acscatal.5b00248.
- [24] S. Derossi, G. Ferraris, S. Fremiotti, E. Garrone, G. Ghiotti, M.C. Campa, V. Indovina, Propane Dehydrogenation on Chromia/Silica and Chromia/Alumina Catalysts, J. Catal. 148 (1994) 36–46. https://doi.org/10.1006/jcat.1994.1183.
- [25] K. Searles, K.W. Chan, J.A. Mendes Burak, D. Zemlyanov, O. Safonova, C. Copéret, Highly Productive Propane Dehydrogenation Catalyst Using Silica-Supported Ga–Pt Nanoparticles Generated from Single-Sites, J. Am. Chem. Soc. 140 (2018) 11674–11679. https://doi.org/10.1021/jacs.8b05378.
- [26] K. Searles, G. Siddiqi, O. V. Safonova, C. Copéret, Silica-supported isolated gallium sites as highly active, selective and stable propane dehydrogenation catalysts, Chem. Sci. 8 (2017) 2661–2666. https://doi.org/10.1039/C6SC05178B.
- [27]H. Jeong, O. Kwon, B.-S. Kim, J. Bae, S. Shin, H.-E. Kim, J. Kim, H. Lee, Highly durable metal ensemble catalysts with full dispersion for automotive applications beyond single-atom catalysts, Nat. Catal. 3 (2020) 368–375. https://doi.org/10.1038/s41929-020-0427-z.
- [28] J.H. Kwak, J. Hu, D. Mei, C.-W. Yi, D.H. Kim, C.H.F. Peden, L.F. Allard, J. Szanyi, Coordinatively Unsaturated Al3+ Centers as Binding Sites for Active Catalyst Phases of Platinum on γ-Al2O3, Science. 325 (2009) 1670–1673. https://doi.org/10.1126/science.1176745.
- [29] J.H. Kwak, J.Z. Hu, D.H. Kim, J. Szanyi, C.H.F. Peden, Penta-coordinated Al3+ ions as preferential nucleation sites for BaO on γ-Al2O3: An ultra-high-magnetic field 27Al MAS NMR study, J. Catal. 251 (2007) 189–194. https://doi.org/10.1016/j.jcat.2007.06.029.
- [30] Z. Lian, C. Si, F. Jan, S. Zhi, B. Li, Coke Deposition on Pt-Based Catalysts in Propane Direct Dehydrogenation: Kinetics, Suppression, and Elimination, ACS Catal. 11 (2021) 9279–9292. https://doi.org/10.1021/acscatal.1c00331.
- [31] K.P. de Jong, Deposition Precipitation, in: Synth. Solid Catal., John Wiley & Sons, Ltd, 2009: pp. 111–134. https://doi.org/10.1002/9783527626854.ch6.
- [32] J.T. Miller, M. Schreier, A.J. Kropf, J.R. Regalbuto, A fundamental study of platinum tetraammine impregnation of silica: 2. The effect of method of preparation, loading, and calcination temperature on (reduced) particle size, J. Catal. 225 (2004) 203–212. https://doi.org/10.1016/j.jcat.2004.04.007.

- [33]D. Leshchev, M. Rakitin, B. Luvizotto, R. Kadyrov, B. Ravel, K. Attenkofer, E. Stavitski, The Inner Shell Spectroscopy beamline at NSLS-II: a facility for in situ and operando X-ray absorption spectroscopy for materials research, J. Synchrotron Radiat. 29 (2022) 1095–1106. https://doi.org/10.1107/S160057752200460X.
- [34] T. Ressler, WinXAS: a Program for X-ray Absorption Spectroscopy Data Analysis under MS-Windows, J. Synchrotron Radiat. 5 (1998) 118–122. https://doi.org/10.1107/S0909049597019298.
- [35] J.J. Rehr, C.H. Booth, F. Bridges, S.I. Zabinsky, X-ray-absorption fine structure in embedded atoms, Phys. Rev. B. 49 (1994) 12347–12350. https://doi.org/10.1103/PhysRevB.49.12347.
- [36] L. Liwu, Z. Tao, Z. Jingling, X. Zhusheng, Dynamic process of carbon deposition on Pt and Pt–Sn catalysts for alkane dehydrogenation, Appl. Catal. 67 (1990) 11–23. https://doi.org/10.1016/S0166-9834(00)84428-0.
- [37]H.N. Pham, A.E. Anderson, R.L. Johnson, K. Schmidt-Rohr, A.K. Datye, Improved Hydrothermal Stability of Mesoporous Oxides for Reactions in the Aqueous Phase, Angew. Chem. Int. Ed. 51 (2012) 13163–13167. https://doi.org/10.1002/anie.201206675.
- [38] H.N. Pham, A.E. Anderson, R.L. Johnson, T.J. Schwartz, B.J. O'Neill, P. Duan, K. Schmidt-Rohr, J.A. Dumesic, A.K. Datye, Carbon Overcoating of Supported Metal Catalysts for Improved Hydrothermal Stability, ACS Catal. 5 (2015) 4546–4555. https://doi.org/10.1021/acscatal.5b00329.
- [39]C. Sun, J. Luo, M. Cao, P. Zheng, G. Li, J. Bu, Z. Cao, S. Chen, X. Xie, A comparative study on different regeneration processes of Pt-Sn/γ-Al2O3 catalysts for propane dehydrogenation, J. Energy Chem. 27 (2018) 311–318. https://doi.org/10.1016/j.jechem.2017.09.035.